ORIGINAL CONTRIBUTION

YJBM

Simultaneously Detection of 50 Mutations at 20 Sites in the *BRAF* and *RAS* Genes by Multiplexed Single-Nucleotide Primer Extension Assay Using Fine-Needle Aspirates of Thyroid Nodules

Aaron A. Stence, Michael P. Gailey, Robert A. Robinson, Chris S. Jensen, and Deqin Ma*

Department of Pathology, University of Iowa Hospitals and Clinics, Iowa City, Iowa

Fine-needle aspiration (FNA†) is commonly used for primary evaluation of thyroid nodules. Twenty to 30 percent of thyroid nodules remain indeterminate after FNA evaluation. Studies show the *BRAF* p.V600E to be highly specific for papillary thyroid carcinoma (PTC), while *RAS* mutations carry up to 88 percent positive predictive value for malignancy. We developed a two-tube multiplexed PCR assay followed by single-nucleotide primer extension assay for simultaneous detection of 50 mutations in the *BRAF* (p.V600E, p.K601E/Q) and *RAS* genes (*KRAS* and *NRAS* codons 12, 13, 19, 61 and *HRAS* 61) using FNA smears of thyroid nodules. Forty-two FNAs and 27 paired formalin-fixed, paraffin-embedded (FFPE) tissues were tested. All *BRAF* p.V600E-positive FNA smears (five) carried a final diagnosis of PTC on resection. *RAS* mutations were found in benign as well as malignant lesions. Ninety-two percent concordance was observed between FNA and FFPE tissues. In conclusion, our assay is sensitive and reliable for simultaneous detection of multiple *BRAF/RAS* mutations in FNA smears of thyroid nodules.

INTRODUCTION

The prevalence of palpable thyroid nodules in the United States is approximately 4 to 7 percent [1]. With examination by high resolution ultrasound, the incidence increases dramatically (19 to 67 percent) [2,3], with many of the additional nodules representing small, incidental lesions that are palpable during physical examination. Although between 5 and 10 percent of palpable nodules are malignant [4], the incidence of malignancy is likely less for small incidental lesions. As the fundamental purpose of nodule evaluation is to determine the probability that a nodule is malignant, additional testing

modalities are necessary to clarify the probability of malignancy and develop a definitive management plan.

Fine-needle aspiration (FNA) is the most commonly used method for further evaluation of palpable and radiologically detected thyroid nodules. While the majority of nodules can be classified definitively as benign or malignant with FNA, up to 20 to 30 percent of aspirated nodules fall into indeterminate categories, including follicular neoplasm (FN), follicular lesion of undetermined significance/atypia of undetermined significance (FLUS/AUS), and suspicious for malignancy [5-7]. Although some of these are due to issues of specimen cellularity and/or other qualitative features that may be clarified by repeat FNA,

*To whom all correspondence should be addressed: Deqin Ma, MD, PhD, Department of Pathology, University of Iowa Hospitals and Clinics, 200 Hawkins Drive, BT6008GH, Iowa City, IA 52242; Tele: 319-384-5700; Fax: 319-356-4916; Email: deqin-ma@uiowa.edu.

†Abbreviations: FNA, fine-needle aspiration; PTC, papillary thyroid carcinomas; FN, follicular neoplasm; FLUS/AUS, follicular lesion of undetermined significance/atypia of undetermined significance; FFPE, formalin-fixed, paraffin-embedded; Snu-PE, single-nucleotide primer extension; LOD, limit of detection; NGS, next generation sequencing; Pap, Papanicolaou.

Keywords: *BRAF*, *RAS*, single nucleotide primer extension assay, cytology smears, thyroid nodules

many of these patients undergo diagnostic thyroid lobectomy that may be followed by completion thyroidectomy if the cytologically indeterminate nodule turns out to be malignant [8].

Alternations in the RAS-RAF-MEK-ERK pathway have been found to be associated with malignant thyroid nodules [9-11]. Mutation in *BRAF* protooncogene has been identified in 50 percent of papillary thyroid carcinomas (PTCs), and the presence of *BRAF* p.V600E mutation is highly specific for PTC (positive predicted value for cancer: 99.3 percent) [12]. *RAS (KRAS, NRAS*, and *HRAS*) mutations are the second most common mutation detected in FNA biopsy samples from thyroid nodules and have a 74 to 88 percent positive predictive value for malignancy [13]. Molecular testing has been shown to improve the accuracy of FNA diagnosis, particularly for nodules with indeterminate cytology [8,14-15] and thus may help with patient management decisions [16].

Multiple test platforms have been developed to detect mutations in *BRAF* and the *RAS* genes. The majority of clinical laboratories are still using formalin-fixed, paraffin-embedded (FFPE) tissue/cell blocks as the sole source for molecular testing. We developed a simple, cost-effective two-tube multiplexed polymerase chain reaction (PCR) assay followed by single-nucleotide primer extension (Snu-PE) assay to simultaneously detect 50 mutations at 20 sites in *BRAF* and the *RAS* gene family. The same diagnostic cytology smears were used for molecular testing, which allows direct visualization of the area of interest and maximizes the utility of FNA materials.

METHODS

This study contains data from a clinical test validation using archived specimens. The study was approved by the Institutional Research Review Committee at the University of Iowa (Iowa City, IA). No informed consent was required.

Case Selection

Forty-two thyroid FNA smears — Romanowsky-type and Papanicolaou (Pap) stained — from 41 patients were selected from archived cytology slides at the Department of Pathology, University of Iowa Hospitals and Clinics (Iowa City, IA). Corresponding FFPE tissues from resection specimens were available from 27 specimens. All cases were reviewed by both surgical pathologists and cytopathologists. Care was taken to conserve a diagnostic slide for the medical record.

DNA Isolation

We targeted only areas with at least 30 percent follicular cells on the FNA smears. Areas with the highest percentage of follicular cells and least amount of contaminating materials (inflammatory cells, debris, blood, and mucin) were marked by a cytopathologist, followed by etching using a diamond-tipped pen on the underside of the slide. The slide was then soaked in xylene until the cov-

erslip could be removed with ease. The de-coverslipped slide was washed in xylene, followed by washing with 95 to 100 percent ethanol. After air-drying, a small amount of matrix capture solution (Pinpoint Slide DNA Isolation, Zymo Research, Irvine, CA) was applied to the desired areas. Tissue bound to the solution was manually microdissected and resuspended in DNA extraction buffer included in the Pinpoint kit, and this was followed by proteinase K digestion at 55°C overnight. After the overnight digestion, the tissue was heat-inactivated at 98°C for 10 minutes followed by 2 minutes on ice. The crude cell lysate was centrifuged (16,000 g × 10 minutes) and the supernatant was directly used for molecular testing.

For FFPE cell blocks/tissues, one hematoxylin and eosin (H&E)-stained slide and 10 unstained sections (6 microns in thickness) were cut. Areas with the highest percentage of tumor (percentage of tumor cells in all cases were above 85 percent) were marked on the H&E slide by a surgical pathologist, and corresponding areas from the unstained slides were manually microdissected using a razor blade. Depending on amount of tissue present, two to 10 sections were used. The paraffin flakes were placed in a 1.5 mL microcentrifuge tube, deparaffinized with 1200 μL of xylene, vortexed, and centrifuged (16,000 g × 5 minutes). The tissue pellet was washed with 1200 μL of 95 percent ethanol twice before proceeding with the extraction. Genomic DNA (gDNA) was isolated from the microdissected FFPE sections using the QIAamp DNA FFPE Tissue Kit (Qiagen, Valencia, CA).

Extracted gDNA from both cytology smears and FFPE tissues was quantified with the Qubit 2.0 fluorometer (Life Technologies, Carlsbad, CA) and the NanoDrop spectrophotometer (Thermo Fisher Scientific, Wilmington, DE). The quality of the DNA was assessed with the ratio of absorbances at 260 and 280 nm. The final volume for DNA from both sources was 60 μl.

PCR Amplification

Exon 15 of the *BRAF* gene; codons 12, 13, 19, and 61 of the *KRAS* gene; codons 12, 13, 61 of the NRAS gene; and codon 61 of the *HRAS* gene were PCR-amplified in two multiplexed reactions using primers as described previously [17-18]. For specimens with lower DNA concentration, the specimens were dried with a vacuum concentrator and resuspended in 5 μl of deionized water. The amplification products were purified using the Qiagen QIAquick PCR Purification Kit (Qiagen) following manufacturer's instructions.

Positive Controls and Cell Lines

One *NRAS* mutant cell line, CRL 1572 (c.35G>A, p. G12D), and two *HRAS* mutant cell lines, CRL-1671 (*c.183G>T*, p.Q61H) and CRL-8083 (*c.182A>G*, p.Q61R), were obtained from ATCC (Manassas, VA). Positive controls for the rest of the mutations were generated by site-directed mutagenesis using the QuikChange® Lightning Site-Directed Mutagenesis Kit (catalog #210518, Stratagene, La Jolla, CA) followed by cloning into plasmids. Leu-

Table 1. Probe sequences for *BRAF* and *RAS* Primer Extension Assay.

Probes	Sequence *(T# = poly "T" primer header)*	Observed bp size	Strand	WT	MT
***BRAF* Probes**					
BRAF V600E	T14 GGT GAT TTT GGT CTA GCT ACA G	46	sense	T	A
BRAF K601Q/E	T21 GGA CCC ACT CCA TCG AGA TT	49	antisense	T	G/C
***KRAS* Probes**					
KRAS pos.34	T30 GGC ACT CTT GCC TAC GCC AC	55	antisense	C	G/A/T
KRAS pos.35	T36 AAC TTG TGG TAG TTG GAG CTG	62	sense	G	C/A/T
KRAS pos.37	T44 CAA GGC ACT CTT GCC TAC GC	67	antisense	C	G/A/T
KRAS pos.38	T49 CTT GTG GTA GTT GGA GCT GGT G	77	sense	G	C/A/T
KRAS pos.57	T54 ATG ATT CTG AAT TAG CTG TAT CGT	84	antisense	C	G/A/T
KRAS pos.181	T63 CTC ATT GCA CTG TAC TCC TCT T	88	antisense	G	C/A/T
KRAS pos.182	T73 CAT TGC ACT GTA CTC CTC T	98	antisense	T	C/G/A
KRAS pos.183	T76 CCT CAT TGC ACT GTA CTC CTC	102	antisense	T	C/G/A
***HRAS* Probes**					
HRAS pos.181	T15 CAT GGC GCT GTA CTC CTC CT	41	antisense	G	C/A/T
HRAS pos.182	T20 GCA TGG CGC TGT ACT CCT CC	49	antisense	T	G/A/C
HRAS pos.183	T5 GCA TGG CGC TGT ACT CCT C	34	antisense	C	G/A/T
***NRAS* Probes**					
NRAS pos.34	T28 CAA ACT GGT GGT GGT TGG AGC A	56	sense	G	C/A/T
NRAS pos.35	T36 CTG GTG GTG GTT GGA GCA G	61	sense	G	C/A/T
NRAS pos.37	T41 GGT GGT GGT TGG AGC AGG T	65	sense	G	C/A/T
NRAS pos.38	T44 GTC AGT GCG CTT TTC CCA ACA	69	antisense	C	G/A/T
NRAS pos.181	T53 CTC ATG GCA CTG TAC TCT TCT T	80	antisense	G	C/A/T
NRAS pos.182	T58 GAC ATA CTG GAT ACA GCT GGA C	85	sense	A	C/G/T
NRAS pos.183	T63 CTC TCA TGG CAC TGT ACT CTT C	91	antisense	T	G/A

cocytes from a healthy donor were used as a negative control.

BRAF (p.V600 and p.K601) and RAS (KRAS, NRAS, and HRAS) Mutation Analysis by Snu-PE

Snu-PE was performed using the SNaPshot Multiplex Kit (Applied Biosystems, Foster City, CA) in a two-tube assay. The approximate sizing locations of individual primers were determined by following the kit protocol from the SNaPshot Primer Focus Kit (Applied Biosystems), which allows separation of mutant peaks from wild-type peaks or non-specific peaks by both size and color. PCR amplification was performed as described above. After PCR amplification, the products were subjected to probe annealing and the addition of a single fluorescently labeled dideoxynucleotide. The primer extension probes were designed with various lengths of deoxythymidine monophosphate homopolymers ranging from 14 to 76 bases to allow discrimination of the products by size (see Table 1 for probe sequences). The probes were designed to be in the sense or antisense direction and end one base 5' of the following positions: *c.1799* and *c.1801* of the *BRAF* gene; *c.34, c.35, c.37, c.38, c.57, c.181, c.182*, and *c.183* of the *KRAS* gene; *c.34, c.35. c.37, c.38, c.181, c.182*, and *c.183* of the *NRAS* gene; and *c.181, c.182*, and *c.183* of the *HRAS* gene. Tube 1 contained BRAF p.V600 and p.K601, and codons 12, 13, 19, and 61 of the *KRAS* gene. Tube 2 included codon 61 of the *HRAS* gene and codons 12, 13, and 61 of the *NRAS* gene. The primer extension products were analyzed by capillary electrophoresis (CE). The limit of detection (LOD) for mutations in all four genes was 5 percent.

Mutation Analysis by Massively Parallel Sequencing

A laboratory-developed/validated next generation sequencing (NGS) panel that can detect hotspot mutations in 10 cancer-related genes (*BRAF, KRAS, NRAS, HRAS, CTNNB, EGFR, FLT3, KIT, PDGFRA*, and *PIK3CA*) was used to confirm some of the Snu-PE findings. Briefly, 20 ng of gDNA was used for preparation of the amplicon libraries using the Ion AmpliSeq™ 2.0 technology (Life Technologies, Carlsbad, CA). The AmpliSeq™ library was clonal amplification by emulsion PCR, followed by simultaneous/parallel sequencing of the clonally amplified DNA templates. The data were analyzed using the Ion Torrent Suite Software (Life Technologies), followed by a laboratory-developed and -validated pipeline. The assay has an analytic sensitivity of 5 percent.

RESULTS

Characteristics of the Snu-PE Assay

The method of extracting gDNA from direct cytology smears (both Romanowsky-type and Pap) was previously

Table 2. Correlation of Molecular Findings with Cytologic and Surgical Pathologic Diagnosis.

Case	FNT Diagnosis	Resection Diagnosis	*BRAF*	*KRAS*	*NRAS*	*HRAS*	Stain	Smear: DNA yield (ng/µl)	FFPE: DNA yield (ng/µl)	Confirmation by NGS	Concordance with FFPE
1	AUS	FVPTC	**p.V600E**	WT	WT	WT	DQ	3.30	3.0	NT	YES
2	AUS	Multinodular hyperplasia	WT	WT	WT	WT	DQ	2.91	111	NT	YES
3	FN	PTC, CV	WT	WT	**p.Q61R**	WT	Pap	0.69	65	YES	YES
4	AUS	Adenomatoid nodule	WT	WT	WT	WT	Pap	0.68	74	YES	YES
5	AUS	FA	WT	WT	WT	WT	DQ	9.78	47	NT	YES
6	HN	Hurthle cell nodule	WT	**p.G12V**	WT	WT	DQ	7.22	88	YES	YES
7	Sus PTC	PTC	WT	WT	WT	WT	DQ	11.00	242	NT	YES
8	Sus PTC	PTC	**p.V600E**	WT	WT	WT	DQ	2.20	22	NT	YES
9	Sus PTC	PTC	WT	WT	WT	WT	DQ	1.48	46	YES	YES
10	Sus PTC	PTC	WT	WT	WT	WT	DQ	10.80	NT	NT	NT
11	FN	FA	WT	WT	WT	WT	DQ	12.50	81	NT	YES
12	FN	FA	WT	WT	WT	WT	DQ	21.20	9.0	NT	YES
13	Sus PTC	PTC	**p.V600E**	WT	WT	WT	DQ	9.0	NT	NT	NT
14	FN	FA	WT	WT	WT	WT	DQ	5.08	221	NT	YES
15	AUS	Adenomatoid nodule	WT	WT	WT	WT	DQ	30.00	47	NT	YES
16	Sus FN	FVPTC	WT	**p.Q61R**	WT	WT	DQ	11.70	80	YES	YES
17	Sus FN	FC	WT	WT	WT	WT	Pap	0.13	45	NT	YES
18	AUS	FA	**Weak p.V600E**	WT	WT	WT	DQ	7.00	NT	NO	NO
19	Sus FN	FA	WT	WT	**p.Q61K**	WT	Pap	0.3	96	NT	YES
20	FN	FA	WT	WT	WT	WT	DQ	23.40	232	NT	YES
21	AUS	FVPTC	WT	WT	WT	WT	DQ	7.00	21	NT	YES
22	Sus FN	FVPTC	**Weak p.V600E**	WT	WT	WT	DQ	20.04	30	NO	NO
23	Sus FN	FVPTC	WT	WT	WT	WT	DQ	5.00	21	NT	YES
24	AUS	Nodular hyperplasia	WT	WT	WT	WT	DQ	2.16	NT	NT	NT
25	Sus FN	Benign nodule	WT	WT	WT	WT	DQ	9.24	NT	NT	NT
26	AUS	FA	WT	WT	WT	WT	DQ	0.20	NT	NT	NT
27	HN	HC	WT	WT	WT	WT	DQ	13.00	NT	NT	NT
28	Sus HN	HC	WT	WT	WT	WT	DQ	2.96	NT	NT	NT
29	Hurthle cell nodule	Hyperplastic nodules with hurthle cell change	WT	WT	WT	WT	DQ	1.62	NT	NT	NT
30	AUS	FC	WT	WT	WT	WT	DQ	0.15	NT	NT	NT
31	HN	PTC	WT	WT	WT	WT	Pap	18.20	NT	NT	NT
32	HN	HC	WT	WT	WT	WT	Pap	4.52	NT	NT	NT
33	AUS	microcarcinoma	WT	WT	WT	WT	Pap	2.06	NT	NT	NT
34	FN	PTC	**p.V600E**	WT	WT	WT	DQ	2.3	14.5	YES	YES
	FN	Nodular hyperplasia	WT	WT	**p.Q61K**	WT	DQ	2.3	250	YES	YES
35	FN	Adenomatoid nodule	WT	WT	**p.Q61R**	WT	DQ	3.04	141	YES	YES
36	FN	PTC	WT	WT	WT	WT	DQ	10.80	NT	NT	NT
37	Hurthle cell lesion	Adenomatoid nodule with Hurthle cell change	WT	WT	**p.Q61R**	WT	DQ	9.52	107	NT	YES
38	FN	Adenomatoid nodule	WT	WT	WT	WT	DQ	5.20	NT	NT	NT
39	FN	FA	WT	WT	**p.Q61R**	WT	DQ	0.12	4.5	YES	YES
40	PTC	FVPTC	**p.V600E**	WT	WT	WT	DQ	0.54	65	NT	YES
41	FN	FVPTC	WT	WT	WT	**p.Q61R**	DQ	12.9	NT	YES	NT

Abbreviations: AUS, atypia of undetermined significance; Dud, suspicious; FVPTC, follicular variant of papillary thyroid carcinoma; CV, columna cell variant; FN, follicular neoplasm; FA, follicular adenoma; FC, follicular carcinoma; HC, Hurthle cell carcinoma; HN, Hurhtle cell neoplasm; WT, wild-type; DQ, Diff-Quick stain; Pap, Papanicolaou stain; FFPE, formalin-fixed, paraffin-embedded; NGS, next generation sequencing; NT, not tested.

validated at our Clinical Laboratory Improvement Amendments (CLIA)-certified molecular pathology laboratory [19]. Genomic DNA was isolated from 42 FNA smears (35 Romanowsky-type and seven Pap). The number and percentage of follicular cells ranged from approximately 200 to 10,000 and 30 to 95 percent, respectively. The total DNA yields ranged from 6.9 ng to 1.65 µg. The DNA yield of FFPE tissue ranged from 0.18 to 14.52 µg.

The sensitivity of the assay was determined by mixing mutant gDNA with wild-type (WT) DNA from previously tested healthy individuals at different dilutions. Mutant cell lines for *NRAS* (one cell line) and *HRAS* (two cell lines) or plasmid DNAs that carry nine different mutations in five sites of *KRAS* codons 12 and 13, and p.V600 and p.K601, of the *BRAF* gene were used. The sensitivity of the assay for all mutations in four genes was 5 percent. A mixture of
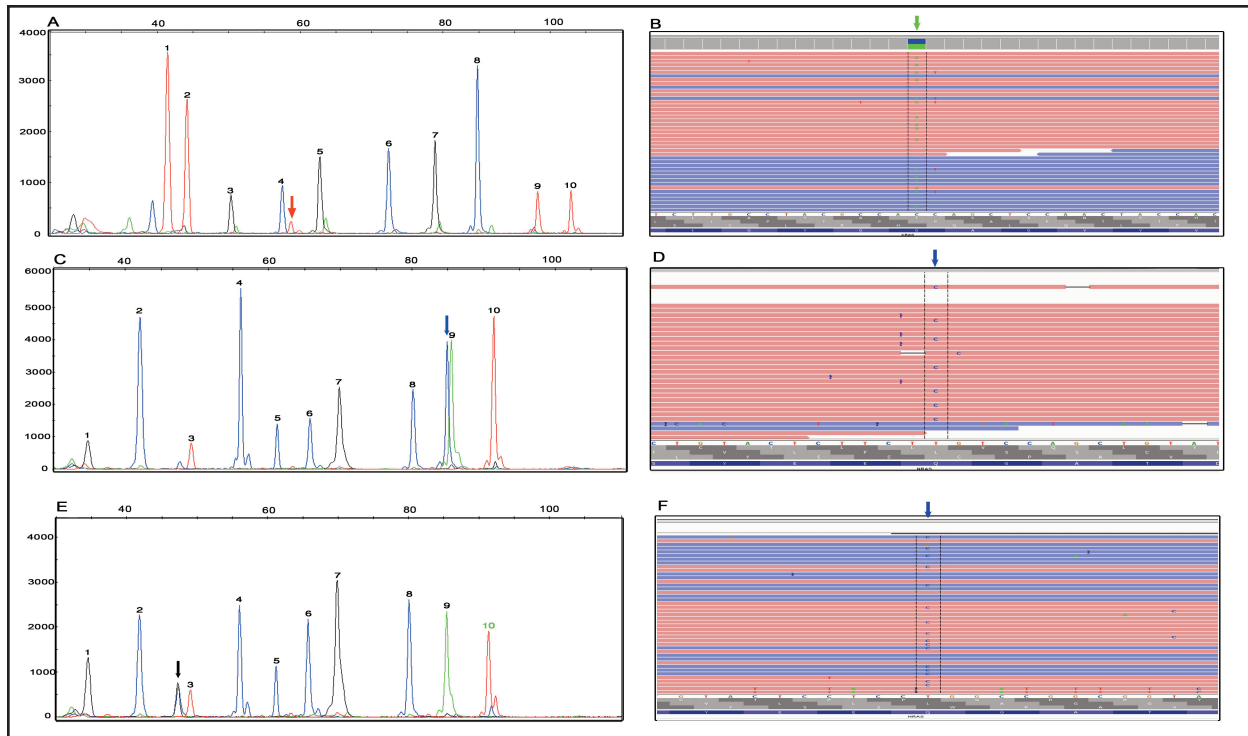
Figure 1. Detection of *RAS* mutations by Snu-PE assay and confirmation by NGS. The mutation analysis for the *RAS* family genes was performed with a 2-tube multiplexed polymerase chain reaction followed by a Snu-PE assay. **A)** *KRAS c.35G>T* (p.G12V) mutation (red peak indicated by the arrow) in a FNA of Hurthle cell nodule (Case 6). Peaks 1 to 10 represent the wild-type alleles at positions *c.1799* and *c.1801* of the *BRAF* gene; and *c.34, c.35, c.37, c.38, c.57, c.181, c.182,* and *c.183* of the *KRAS* gene, respectively. **B)** The presence of *KRAS c.35G>T* mutation in A (green arrow, reverse strand) was confirmed by NGS. Integrative genomic viewer (IGV). **C)** *NRAS c.182A>G* (p.Q61R) mutation (blue peak indicated by the arrow) in FNA smear of an adenomatoid nodule (case #35). **D)** NGS confirmation of *NRAS c.182A>G* mutation (blue arrow, reverse strand) detected in C. IGV view. **E)** *HRAS c.182A>G* (p.Q61R) mutation (black peak indicated by the arrow, antisense probe) in a follicular variant of PTC (Case 41). **F)** NGS confirmation of *HRAS c.182A>G* mutation (blue arrow, reverse strand) detected in E. IGV view. Peaks 1-10 in C and E represent the wild-type alleles at positions *c. 183, c.181,* and *c.182* of *HRAS* and *c.34, c.35, c.37, c.38, c.181*, *c.182*, and *c.183* of the *NRAS* gene, respectively. Labels on the x-axis are the size markers. Labels on the y-axis indicate the intensity of the fluorescence, which can be used as a relative assessment of the mutant sequence represented in the sample. Ref, reference sequence; FNA, fine-needle aspiration; NGS, next generation sequencing; Snu-PE, single-nucleotide primer extension; PTC, papillary thyroid carcinoma.

DNAs with different known mutations in *BRAF/KRAS* and *HRAS* or *NRAS* genes, each representing a final mutant allele frequency of 5 percent, was included as a positive control and sensitivity control in each run.

Detection of BRAF and KRAS/NRAS/HRAS Mutations by Snu-PE

Mutation analysis for *BRAF* p.V600E, p.K601E, p.K601Q; *KRAS* codons 12, 13, 19, and 61; NRAS codons 12, 13, and 61; and *HRAS* codon 61 was performed using gDNAs extracted from both direct cytology smears as well as FFPE tissues. Seven *BRAF* p.V600E mutations, two KRAS mutations, six *NRAS* mutations, and one *HRAS* mutations were identified in 16 of 42 FNA smears (38 percent) (Table 2). Twelve mutations (four *BRAF*, two *KRAS*, and six *NRAS*) were identified in 27 FFPE specimens (44 percent). Two cases (18 and 22) had a weak *BRAF* p.V600E peak in FNA smears but not in corresponding FFPE tissues. Both *BRAF* p.V600E and *NRAS* p.Q61K

mutations were found in the cytology smear in Case 34. Coexistent PTC and hyperplastic nodule were identified on the same block in the resection specimen. Areas with PTC and nodular hyperplasia were microdissected separately from FFPE tissues and tested for *BRAF/RAS* mutations. A *BRAF* p.V600E mutation was identified in PTC and a *NRAS* p.Q61K mutation was found in the hyperplastic nodule. Representative Snu-PE findings of a *KRAS* p.G12V mutation in a Hürthle cell nodule (Case 6), a *NRAS* p.Q61R mutation in an adenomatoid nodule (Case 35), and a *HRAS* mutation in a follicular variant of PTC (FVPTC) (Case 41) are shown in Figure 1 (A, C, and E). The mutant peak (black) in 1E overlapped with a non-specific peak (blue) but was the right color and size based on SNaPshot Primer Focus Kit.

Confirmation of Snu-PE Findings by NGS

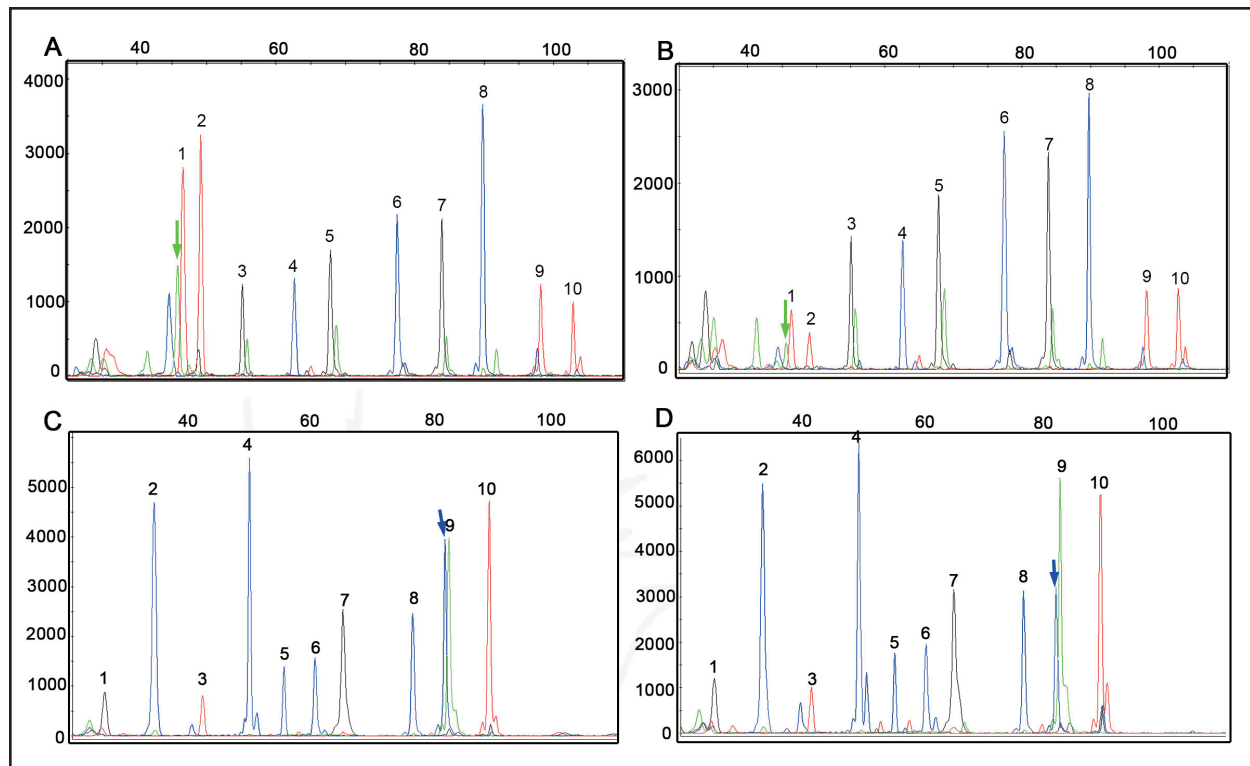A laboratory-developed and validated NGS panel, which includes all *BRAF* and *RAS* mutations in our Snu-

Figure 2. *BRAF* and *NRAS* mutations detected by Snu-PE in FNA smears and paired FFPE tissues. **A)** *BRAF c.1799T>A* (p.V600E) mutation (green peak indicated by the arrow) detected in a follicular variant of PTC (Case 40). **B)** Paired FFPE tissue of Case 40 in A. Peaks 1-10 in A and B represent wild-type alleles at positions *c.1799* and *c.1801* of the *BRAF* gene and *c.34, c.35, c.37, c.38, c.57, c.181, c.182,* and *c.183* of the *KRAS* gene, respectively. **C)** *NRAS c.182A>G* (p.Q61R) mutation (blue peak indicated by the arrow) in a second case of follicular variant of PTC (Case 3). **D)** Paired FFPE tissue of Case 3 in C. Peaks 1-10 in C and D represent the wild-type alleles at positions *c. 183, c.181,* and *c.182* of *HRAS* and *c.34, c.35, c.37, c.38, c.181, c.182*, and *c.183* of the *NRAS* gene, respectively. Labels on the x-axis are the size markers. Labels on the y-axis indicate the intensity of the fluorescence, which can be used as a relative assessment of the mutant sequence represented in the sample. The blue peak at *c.1799* and the green peaks at *c.34, c.37, c.57* and *c.181* in (A) and (B) are artifacts which were not present in primer focus. SNu-PE, single-nucleotide primer extension; FNA, fine-needle aspiration; FFPE, formalin-fixed, paraffin embedded.

PE assay, was used to confirm findings of the Snu-PE assay. Eight positive case that include all the cases with low mutant allele frequency and sufficient remaining DNA and two negative cases were tested. Representative results of NGS confirmation are shown in Figure 1 (B, D, and F). The weak *BRAF* p.V600E peaks in the FNA smear of Cases 18 and 22 were not identified by NGS. A low level (4.9 percent) of *NRAS* p.Q61R mutation was identified in the FNA smear of Case 39, and an even lower frequency (2.5 percent) was seen in the corresponding FFPE tissue. The presence of this mutation was confirmed by NGS at an allele frequency of 4.1 percent in FNA smear of Case 39 but not in the paired FFPE tissue. The *BRAF* p.V600E mutation in Cases 18 and 22 FNA smears were considered as false positives, but the *NRAS* mutation in the Case 39 FNA smear was considered as a true positive.

Correlation of Cytology Smear with FFPE Tissue

DNAs from 27 cases with available corresponding FFPE tissue were tested by Snu-PE in parallel. Concordance between cytology smears and FFPE tissue was found in 25 cases (92.5 percent, n = 17). Representative

Snu-PE findings in cytology smears and corresponding FFPE tissues were shown in Figure 2.

Correlation of Molecular Findings with Pathologic Diagnosis of Thyroid Nodules

The cytologic diagnosis of the 42 FNA cases included in this study were 11 atypia of undetermined significance/follicular lesion of undetermined significance (AUS/FLUS), 25 follicular neoplasm (FN)/suspicious for FNs, five suspicious for malignancy and one PTC. The initial cytologic diagnosis for the 5 *BRAF* V600E-positive cases were AUS (1), suspicious for FN (1), suspicious for PTC (2), and PTC (1), all of which carried a final diagnosis of PTC on resection. The six *NRAS*-positive cases were FN/suspicious for FN (4), follicular lesion (1), and Hürthle cell lesion (1). The surgical pathology diagnoses were follicular variant of papillary thyroid carcinoma (FVPTC) (1), follicular adenoma (FA) (2), and benign follicular nodules (3). One *KRAS*-positive case had a FNA and surgical pathology diagnosis of FN (Hürthle cell) and Hürthle cell nodule, respectively. The second *KRAS*-positive case had a FNA diagnosis of suspicious for FN and tissue di-

Table 3. Risk of Malignancy and Benign Lesions Associated with FNA Diagnosis and Mutation.

FNA Diagnostic Category	Malignancy Associated with FNA Diagnosis	Malignancy Associated with Mutations	Benign Lesions Associated with Mutation
FLUS/AUS	36% (n=11)	25% (n=4)	0 (n=7)
FN or Suspicious for FN	48% (n=25)	33% (n=12)	46% (n=13)
Suspicious for Malignancy	100 % (n=5)	40% (n=5)	0 (n=0)
Malignant	100% (n=1)	100% (n=1)	0 (n=0)
Total	52% (n=42)	66% (n=22)	30% (n=20)

Abbreviations: FLUS/AUS, follicular lesion of undetermined significance/atypia of undetermined significance (FLUS/AUS); FN, follicular neoplasm.

agnosis of FVPTC. The only *HRAS*-positive case was diagnosed as FN by FNA and FVPTC on resection. The correlation of molecular findings with cytologic and histologic diagnosis is summarized in Table 2. The risk of malignancy and benign lesions associated with FNA diagnosis and mutation is summarized in Table 3.

DISCUSSION

Molecular testing for follicular lesions of the thyroid has recently gained attraction and can help direct clinical and surgical management in a subset of thyroid nodules [8,14-16]. The management for obviously malignant and benign thyroid lesions is usually straightforward. However, for indeterminate follicular lesions, patients may first undergo lobectomy, followed by completion thyroidectomy if necessary. Nikiforov et al. [8,14-16] proposed the role of molecular oncology tests on indeterminate thyroid lesions and showed that the presence of *BRAF* p.V600E mutation was highly specific for PTC. Although *RAS* gene mutations can also be seen in benign conditions such as FAs and adenomatoid nodules, they carry a 74 to 88 percent positive predictive value for malignancy [14,16,19].

In the majority of laboratories, molecular tests are only performed on FFPE cell blocks derived from aspirate materials. The diagnosis of thyroid nodules by FNA rarely/never requires cell blocks. The only purpose for the preparation of cell block is for molecular analysis. A pitfall of cell block is the inability to evaluate cellularity of this material on-site, and many times there is insufficient tissue in the block. When this situation arises, a decision has to be made whether to take the patient back for repeat FNA or for a more invasive procedure. Cytologic smears almost always contain sufficient material for diagnosis and are a unique reservoir of DNA for molecular testing. We recently demonstrated that DNAs from direct cytology smears could be used on multiple platforms for molecular oncology testings [19]. In the current study, amplifiable gDNA was extracted from all 42 FNA smears. The low DNA yield from some smears was due to the paucity of cells on the slides.

Twenty-seven FNA cases had paired FFPE tissues from surgical resections. Discordance was seen in two cases. Cases 18 and 22 had a low a level of *BRAF* p.V600E (around 3 percent of WT allele) in FNA smears using Snu-PE, but not in paired FFPE tissues. This mutation was not detected by NGS in either FNA smear or paired FFPE tissues. The tumor percentage was over 50 percent in the cytology smear and 85 percent in FFPE tissue. A much higher mutant allele frequency is expected if the mutation is true. In addition, the LOD of the assay is 5 percent. Mutant peaks below LOD could represent nonspecific background peak. These two FNA smears were, therefore, considered as false positives. The third case (39) had a weak *NRAS* p.Q61R mutation from the tested FNA smear with mutant content of 4.9 percent by Snu-PE and allele frequency of 4.1 percent by NGS. The mutant had an allele frequency of 2.5 percent in the FFPE tissue by Snu-PE but was detected by NGS. This case most likely represents a true-positive finding. We have observed that DNA extracted from cytology preparations seemed to have better quality on the basis of the relative mutant allele present in the cytology specimens [19]. The discrepancy between cytology smear and FFPE tissue could also be due to the presence of inhibitory factors in the FFPE tissue. The risk of PCR contamination also should be taken into consideration when working with small number of cells, especially using sensitive test platforms such as NGS and our Snu-PE assay. For cases with mutation peaks below or at the LOD, especially when the tumor percentage was high, we routinely confirm the Snu-PE findings by an alternative method of similar or higher sensitivity and correlate them with the tumor percentage and pathologic diagnosis.

In our small cohort, we detected 14 mutations in 42 FNA smears from 41 patients. The case with co-existing PTC and hyperplastic nodule (No. 34) had two different mutations: the *BRAF* p.V600E mutation was only seen in PTC, and the *NRAS* mutation was identified in the benign follicular hyperplasia. The overall mutation frequency was 33 percent (n = 42). Thirty-eight percent (n = 21) of the malignancies had *BRAF* or *RAS* mutations. In benign le-

sions, the frequency of mutation was 25 percent (n = 20) (Table 3). The positive predictive value of *BRAF* V600E for PTC was 100 percent, consistent with the reports in the literature [8,14-16]. *RAS* mutations were associated with malignant as well as benign follicular lesions. The predicted value of *RAS* mutation for malignancy was lower than reported in the literature, which is most likely due to the limited number of cases in this study.

Multiple test platforms with different LODs are available in our laboratory for the detection of *BRAF* and *RAS* mutations. Sanger sequencing has been considered the gold standard for detection of point mutations and small deletion/duplications. It is labor-intensive and has a low analytical sensitivity of 20 percent. We also have two NGS platforms that are more sensitive than Sanger but have a longer turn-around time and higher cost. Our Snu-PE assay requires a minimum of 6 ng input gDNA. When probes were carefully designed in sense and anti-sense directions and of various lengths, we were able to detect 50 mutations at 20 sites, which include the most commonly mutated sites in *BRAF* and the *RAS* gene family. The analytic sensitivity of the assay is 5 percent, similar to our NGS platforms. The test has a quick turn-around time and a direct cost of less than $150. It is not only useful for mutation detection in thyroid FNA nodules; it can also be used to determine the eligibility of patients with colorectal carcinoma or malignant melanoma, which commonly harbor *BRAF* p.V600E or *RAS* mutations, for targeted therapies and as a confirmatory test for low level of mutations identified by Sanger sequencing and NGS.

The limitation of this assay is its inability to detect dinucleotide changes in the *BRAF* gene. This is less of a problem in thyroid cancers, since almost all *BRAF* mutations in PTC are p.V600E, with mutations in other *BRAF* codons exceedingly rare. NGS or Sanger sequencing can be used to confirm the findings when double mutant peaks are seen.

In conclusion, our study confirms that the FNA smear from thyroid nodules is a reliable source of DNA for mutation analysis of *BRAF* and *RAS* genes. Our laboratory-developed Snu-PE assay worked well on DNA isolated from both Romanowsky-type and Pap stained slides. It is simple, cost-effective, and has a short turn-around time. This approach allows molecular assays to be performed on specific cells of interest and maximizes the utility of FNA materials. It may also save patients from an additional, unnecessary procedure.

REFERENCES

1. Welker MJ, Orlov D. Thyroid nodules. Am Fam Physician. 2003; 67(3):559-66.
2. Mazzaferri EL. Thyroid cancer in thyroid nodules: finding a needle in the haystack. Am J Med. 1992; 93(4):359-62.
3. Tan GH, Gharib H. Thyroid incidentalomas: management approaches to nonpalpable nodules discovered incidentally on thyroid imaging. Ann Intern Med. 1997;126(3):226-31.
4. Brito JP, Yarur AJ, Prokop LJ, McIver B, Murad MH, Montori VM. Prevalence of thyroid cancer in multinodular goiter versus single nodule: a systematic review and meta-analysis. Thyroid. 2013;23(4):449-55.
5. Cibas ES, Ali SZ. The Bethesda System For Reporting Thyroid Cytopathology. Am J Clin Pathol. 2009;132(5):658-65.
6. Ohori NP, Schoedel KE. Variability in the atypia of undetermined significance/follicular lesion of undetermined significance diagnosis in the Bethesda System for Reporting Thyroid Cytopathology: sources and recommendations. Acta Cytol. 2011;55(6):492-8.
7. Baloch ZW, LiVolsi VA, Asa SL, Rosai J, Merino MJ, Randolph G, et al. Diagnostic terminology and morphologic criteria for cytologic diagnosis of thyroid lesions: a synopsis of the National Cancer Institute Thyroid Fine-Needle Aspiration State of the Science Conference. Diagn Cytopathol. 2008;36(6):425-37.
8. Nikiforov YE, Yip L, Nikiforova MN. New strategies in diagnosing cancer in thyroid nodules: impact of molecular markers. Clin Cancer Res. 2013;19(9):2283-8.
9. Kimura ET, Nikiforova MN, Zhu Z, Knauf JA, Nikiforov YE, Fagin JA. High prevalence of BRAF mutations in thyroid cancer: genetic evidence for constitutive activation of the RET/PTC-RAS-BRAF signaling pathway in papillary thyroid carcinoma. Cancer Res. 2003;63(7):1454-7.
10. Frattini M, Ferrario C, Bressan P, Balestra D, De Cecco L, Mondellini P. Alternative mutations of BRAF, RET and NTRK1 are associated with similar but distinct gene expression patterns in papillary thyroid cancer. Oncogene. 2004;23(44):7436-40.
11. Nikiforova MN, Lynch RA, Biddinger PW, Alexander EK, Dorn GW 2nd, Tallini G, et al. RAS point mutations and PAX8-PPAR gamma rearrangement in thyroid tumors: evidence for distinct molecular pathways in thyroid follicular carcinoma. J Clin Endocrinol Metab. 2003;88(5):2318-26.
12. Nikiforov YE, Nikiforova MN. Molecular genetics and diagnosis of thyroid cancer. Nat Rev Endocrinol. 2011;7(10):569-80.
13. Bhaijee F, Nikiforov YE. Molecular analysis of thyroid tumors. Endocr Pathol. 2011;22(3):126-33.
14. Nikiforov YE, Steward DL, Robinson-Smith TM, Haugen BR, Klopper JP, Zhu Z, et al. Molecular testing for mutations in improving the fine-needle aspiration diagnosis of thyroid nodules. J Clin Endocrinol Metab. 2009;94(6):2092-8.
15. Ohori NP, Nikiforova MN, Schoedel KE, LeBeau SO, Hodak SP, Seethala RR, et al. Contribution of molecular testing to thyroid fine-needle aspiration cytology of "follicular lesion of undetermined significance/atypia of undetermined significance". Cancer Cytopathol. 2010;118(1):17-23.
16. Nikiforov YE, Ohori NP, Hodak SP, Carty SE, LeBeau SO, Ferris RL, et al. Impact of mutational testing on the diagnosis and management of patients with cytologically indeterminate thyroid nodules: a prospective analysis of 1056 FNA samples. J Clin Endocrinol Metab. 2011;96(11):3390-7.
17. Lurkin I, Stoehr R, Hurst CD, van Tilborg AA, Knowles MA, Hartmann A, et al. Two multiplex assays that simultaneously identify 22 possible mutation sites in the KRAS, BRAF, NRAS and PIK3CA genes. PLoS One. 2010;5(1):e8802.
18. Gailey MP, Stence AA, Jensen CS, Ma D. Multiplatform comparison of molecular oncology tests performed on cytology specimens and formalin-fixed, paraffin-embedded tissue. Cancer Cytopathol. 2015;123(1):30-9.
19. Cantara S, Capezzone M, Marchisotta S, Capuano S, Busonero G, Toti P, et al. Impact of proto-oncogene mutation detection in cytological specimens from thyroid nodules improves the diagnostic accuracy of cytology. J Clin Endocrinol Metab. 2010;95(3):1365-9.